

## Quantum-electrodynamics corrections in pionic hydrogen

S. Schlessler,<sup>1,\*</sup> E.-O. Le Bigot,<sup>1</sup> P. Indelicato,<sup>1,†</sup> and K. Pachucki<sup>2</sup>

<sup>1</sup>*Laboratoire Kastler Brossel, École Normale Supérieure, CNRS, Université Pierre et Marie Curie-Paris 6, Case 74, 4 place Jussieu, F-75005 Paris, France*

<sup>2</sup>*Faculty of Physics, University of Warsaw, Hoża 69, PL-00-681 Warsaw, Poland*

(Received 25 August 2009; revised manuscript received 18 May 2011; published 21 July 2011)

We investigate all pure quantum-electrodynamics corrections to the  $np \rightarrow 1s$ ,  $n = 2-4$  transition energies of pionic hydrogen larger than 1 meV, which requires an accurate evaluation of all relevant contributions up to order  $\alpha^5$ . These values are needed to extract an accurate strong interaction shift from experiment. Many small effects, such as second-order and double vacuum polarization contribution, proton and pion self-energies, finite size and recoil effects are included with exact mass dependence. Our final value differs from previous calculations by up to  $\approx 11$  ppm for the  $1s$  state, while a recent experiment aims at a 4 ppm accuracy.

DOI: [10.1103/PhysRevC.84.015211](https://doi.org/10.1103/PhysRevC.84.015211)

PACS number(s): 36.10.Gv, 12.20.Ds, 13.75.Gx, 31.30.jf

### I. INTRODUCTION

Pion-nucleon scattering lengths are quantities of fundamental importance in low-energy hadronic physics. For the  $1s$  state of pionic hydrogen ( $\pi\text{H}$ ), the low energy scattering lengths at threshold  $a_{\pi^-p \rightarrow \pi^-p}$  and  $a_{\pi^-p \rightarrow \pi^0n}$  are connected to  $\epsilon_{1s}$  and  $\Gamma_{1s}$ , the hadronic shift and broadening, through Deser formula [1]

$$\frac{\epsilon_{1s}}{E_{1s}} = -\frac{4}{r_B} a_{\pi^-p \rightarrow \pi^-p} (1 + \delta_\epsilon), \quad (1)$$

$$\frac{\Gamma_{1s}}{E_{1s}} = \frac{8Q_0}{r_B} \left(1 + \frac{1}{P}\right) [a_{\pi^-p \rightarrow \pi^0n} (1 + \delta_\Gamma)]^2, \quad (2)$$

where  $E_{1s}$  is the  $1s$  binding energy. The Bohr radius  $r_B$  is given by

$$r_B = \frac{1}{\mu\alpha Z}, \quad (3)$$

where  $\alpha \approx 1/137.036$  is the fine structure constant and  $Z$  the atomic number. The quantities  $\delta_\epsilon$  and  $\delta_\Gamma$  are corrections due to the distortion of the pion wave function by the strong interaction,  $Q_0 = 0.142 \text{ fm}^{-1}$  is the momentum of the  $\pi^0$  in the center-of-mass system and  $P = 1.546 \pm 0.009$  is the Panofski ratio of scattering amplitudes  $a_{\pi^-p \rightarrow \pi^0n}$  and  $a_{\pi^-p \rightarrow \gamma n}$ , which is derived from experiment [2].

Determination of accurate values of the scattering length allow for tests of chiral perturbation theory—the low energy approach to QCD—in particular for the extraction of chiral symmetry breaking parameters [3–6] as well as for tests of the other approaches [7–10]. The strong interaction shift  $\epsilon_{1s}$  is obtained by comparing theoretical, pure QED transition energies to the measured  $np \rightarrow 1s$  ones. There are many issues involved in the derivation of the physically meaningful scattering amplitudes from the experimentally measurable parameters  $\epsilon_{1s}$  and  $\Gamma_{1s}$ . These issues are mainly connected to the accuracy with which one can disentangle QED and QCD

contributions (see, e.g., [6,11] for recent reviews). In the case of  $a_{\pi^-p \rightarrow \pi^-p}$ , the QED/QCD separation is present in both the extraction of  $\epsilon_{1s}$  from experimental transition energies and in the evaluation of  $\delta_\epsilon$ . The strong interaction shift is a correction of order  $\alpha^3$  to the usual Coulomb binding energy of the  $1s$  level. It was evaluated in leading order in chiral perturbation theory [3] and in next to leading order in [5]. The ground state energy shift is written as [3]

$$\epsilon_{1s} = -2\alpha^3 \mu^2 \mathcal{A} \{1 - 2\alpha(\ln \alpha - 1)\mu \mathcal{A}\} + \dots \quad (4)$$

in terms of the  $\pi^-p \rightarrow \pi^-p$  scattering amplitude at threshold  $\mathcal{A}$ . Here  $\frac{1}{\mu} = \frac{1}{m_\pi} + \frac{1}{m_p}$  is the reduced mass,  $m_\pi$ ,  $m_p$  denoting the charged pion and proton masses, respectively. The scattering amplitude at threshold is connected to the isospin-invariant amplitudes  $a_{0+}^+$  and  $a_{0+}^-$  as

$$\mathcal{A} = a_{0+}^+ + a_{0+}^- + \epsilon, \quad (5)$$

where  $\epsilon$  is the isospin-symmetry breaking term due to the electromagnetic interaction. The evaluation of  $\epsilon$  is required to derive  $a_{0+}^+$  and  $a_{0+}^-$  from experiment. The scattering length  $a_{0+}^+$  and  $a_{0+}^-$  are calculated in an isospin-symmetric theory with no electromagnetic interaction and identical masses for the up and down quarks. With this convention one obtains at order  $\mathcal{O}(p^2)$  [3]

$$\epsilon = \frac{m_p}{8\pi(m_p + m_\pi)F_\pi^2} \{8c_1(m_\pi^2 - m_{\pi^0}^2) - 4e^2 f_1 - e^2 f_2\}, \quad (6)$$

where  $m_{\pi^0}$  is the mass of the neutral pion,  $e$  the electric charge,  $F_\pi = 92.4 \text{ MeV}$  the pion decay constant, and  $c_1$ ,  $f_1$ ,  $f_2$  are the low-energy constants of the phenomenological chiral pion-nucleon interaction Lagrangian. Two of the low-energy constants  $c_1 = -0.9_{-0.5}^{+0.2} \text{ GeV}^{-1}$  [6] and  $e^2 f_2 = -(0.97 \pm 0.38) \text{ MeV}$  [6] can be derived from experiment. The determination of  $f_1$  value, however, is more problematic and leads to the largest uncertainty in the determination of  $a_{0+}^+$  and  $a_{0+}^-$  from  $\epsilon_{1s}$  [5,6]. An uncertainty of 100 MeV represents a contribution to  $\epsilon_{1s}$  of 0.015 eV. Both  $c_1$  and  $f_1$  however, are also present in the pionic deuterium energy shift and can be eliminated in the determination of the isospin symmetric

\*Present address: KVI, Theory Group, University of Groningen, 9747 AA Groningen, The Netherlands.

†paul.indelicato@lkb.ens.fr

scattering length [11,12]. The deuterium shift was measured in several experiments [13–15].

The most accurate present experimental values from pionic hydrogen are  $\epsilon_{1s} = -7.108 \pm 0.013(\text{stat.}) \pm 0.034(\text{syst.})$  eV and  $\Gamma_{ns} = 0.868 \pm 0.040(\text{stat.}) \pm 0.038(\text{syst.})$  eV [16,17]. A recent experiment [18] at the Paul Scherrer Institute aims at a  $\approx 4$  ppm accuracy ( $\approx 0.01$  eV) on transition energies, leading to a determination of the strong interaction shift to better than 1%, if compared to accurate QED results. In this work, we evaluate all QED contributions to the  $1s$  and  $np$ ,  $n = 2-4$  level energies up to order  $\alpha^4$  and all contributions to order  $\alpha^5$  that correspond to purely electromagnetic interaction.

This paper follows the approach used in [19] for muonic hydrogen. All formulas are valid for any state and could be applied to any spin-1/2–spin-0 system, composed of two finite sized particles with masses of the same order of magnitude, in which case both particles must be treated on the same footing, with exact mass dependence. We start from the Breit-Pauli Hamiltonian, which includes the main relativistic and recoil corrections, and accounts for the anomalous magnetic moment of the proton. In addition we calculate leading, double and second order vacuum polarization contributions, relativistic corrections to the leading vacuum polarization term, mixed finite size-vacuum polarization diagrams, particles self-energies, and the part of the two-photon exchange that can be safely traced back to pure electromagnetic interaction. The main limitation in accuracy of the present work is due to uncertainties in the rms charge radius of the proton and pion, and in the pion mass. The fundamental constants and the proton mass are taken from Ref. [20], while the pion mass [139.57018(35) MeV] and charge radius [0.672(8) fm] come from [21]. The situation in what concerns the proton radius is at the moment complicated. There is a recent very accurate value from muonic hydrogen 0.84184(67) fm [22], that is 5 standard deviations away from the one obtained from hydrogen 0.8768(69) fm [20] and from the most recent electron-proton elastic scattering 0.879(8) fm [23]. Here we use the muonic hydrogen value, as the pion and muon mass are close, and whatever effect is at play in this large discrepancy, must be more likely to be identical between muonic and pionic hydrogen.

## II. QED CALCULATION

### A. Breit equation including Darwin term and magnetic moment

The Breit-Pauli Hamiltonian for our system is [24,25]  $H_{\text{BP}} = H_0 + \delta H + V^{\text{BP}}$  with

$$H_0 = \frac{p^2}{2\mu} - \frac{Z\alpha}{r}, \quad \delta H = -\frac{p^4}{8m_\pi^3} - \frac{p^4}{8m_p^3}, \quad (7)$$

$$V^{\text{BP}} = \frac{\pi Z\alpha}{2} \frac{1}{m_\pi^2} \delta^3(r) - \frac{Z\alpha}{2m_p m_\pi} p^i \frac{1}{r} \left( \delta_{ij} + \frac{r_i r_j}{r^2} \right) p^j + \frac{Z\alpha}{r^3} \left( \frac{1+2\kappa}{4m_p^2} + \frac{1+\kappa}{2m_p m_\pi} \right) (\mathbf{r} \times \mathbf{p}) \cdot \boldsymbol{\sigma} \quad (8)$$

$$+ \frac{2}{3} \pi Z\alpha (\langle r_\pi^2 \rangle + \langle r_p^2 \rangle) \delta^3(r). \quad (9)$$

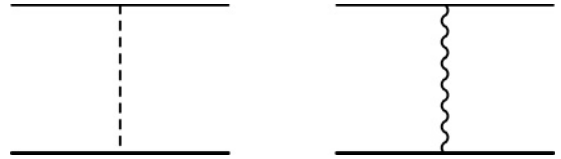


FIG. 1. Diagrams corresponding to the Breit-Pauli Hamiltonian. Dashed lines correspond to the Coulomb interaction, wavy lines to the magnetic interaction and plain thin and thick lines to the lepton or proton wave functions, respectively.

Here  $\langle r_\pi^2 \rangle$ ,  $\langle r_p^2 \rangle$  are the mean square charge radii of the pion and proton,  $\kappa$  is the proton magnetic moment anomaly,  $\boldsymbol{\sigma}$  are Pauli matrices and  $Z$  is the nuclear charge, which is used to distinguish proton and pion contributions. The corresponding QED diagrams are shown in Fig. 1. We note that the pion Darwin term,  $\frac{1}{m_\pi^2} \delta^3(r)$  is absent because the spin of the pion is zero. The known  $\frac{\pi Z\alpha}{2} \frac{(2\kappa)}{m_p^2} \delta^3(r)$  magnetic anomaly correction to the first term in Eq. (8) is in this case included in the proton charge distribution (9), when provided by bound-state measurements [26,27], from which is derived the proton charge radius [22]. The corresponding energies for each contribution can be found in Ref. [25] for example.

A complete relativistic treatment of the pion bound states, in the nonrecoil approximation, can be done in the framework of the Klein-Gordon equation. The corresponding energy is given by the well-known expression

$$E_{\text{KG}}(Z, n, l) = \left[ \left( 1 + \frac{(Z\alpha)^2}{(n-l-\frac{1}{2} + \sqrt{(l+\frac{1}{2})^2 - (Z\alpha)^2})^2} \right)^{-\frac{1}{2}} - 1 \right] \mu c^2, \quad (10)$$

which can be expanded in powers of  $Z\alpha$  as

$$E_{\text{KG}}(Z, n, l) = -\frac{(Z\alpha)^2}{2n^2} \mu c^2 + \left( \frac{3}{8n^4} - \frac{1}{(2l+1)n^3} \right) (Z\alpha)^4 \mu c^2 + \mathcal{O}[(Z\alpha)^6]. \quad (11)$$

The two first terms of this expansion are included in the solutions of Eqs. (7) and (8). We include the sum of all higher-order terms in our result for completeness.

### B. Vacuum polarization corrections

The electron vacuum polarization modifies the effective electromagnetic interaction. Because of the relatively large pion mass, diagrams with vacuum polarization loops dominate among QED corrections, while the self-energy is very small, in contrast to electronic atoms. The vacuum polarization can be evaluated by modifying the photon propagator. In leading order, it corresponds to the replacement:

$$-\frac{g_{\mu\nu}}{k^2} \rightarrow -\frac{g_{\mu\nu}}{k^2} [1 - \bar{\omega}(k^2)]. \quad (13)$$

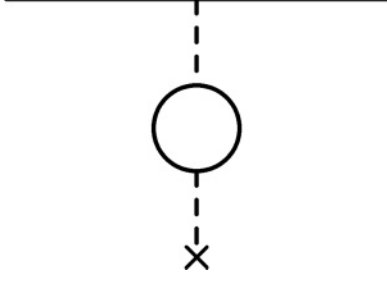


FIG. 2. Diagram corresponding to the vacuum polarization at one loop (Uehling potential). Dashed lines correspond to the Coulomb interaction, plain lines to the electron wave function, and the cross to the interaction with the nuclear charge.

At the one-loop level,  $\bar{\omega}$  is given by [28]:

$$\bar{\omega}(k^2) = \frac{\alpha}{\pi} k^2 \int_4^\infty d(q^2) \frac{1}{q^2(m_e^2 q^2 - k^2)} u(q^2), \quad (14)$$

with

$$u(q^2) = \frac{1}{3} \sqrt{1 - \frac{4}{q^2}} \left(1 + \frac{2}{q^2}\right). \quad (15)$$

This leads to the effective interaction potential (Fig. 2),

$$V_{\text{vp}}(r) = -\frac{Z\alpha}{r} \frac{\alpha}{\pi} \int_4^\infty \frac{d(q^2)}{q^2} e^{-m_e q r} u(q^2), \quad (16)$$

known as the Uehling potential [29]. The corresponding energy shift in the first order is

$$E_{nl} = \langle \phi_{nl} | V_{\text{vp}} | \phi_{nl} \rangle = \int d^3 r V_{\text{vp}}(r) |\phi_{nl}(\mathbf{r})|^2, \quad (17)$$

where  $\phi_{nl}(\mathbf{r})$  is the Schrödinger-Coulomb wave function [30], which depends on the reduced mass  $\mu$ . Replacing Eq. (16) in Eq. (17) leads to

$$E_{nl} = -Z\alpha \frac{\alpha}{\pi} \int_4^\infty \frac{d(q^2)}{q^2} u(q^2) \int dr e^{-m_e q r} r R_{nl}^2(r), \quad (18)$$

where the integral over  $r$  is performed analytically and  $R_{nl}$  is the radial part of  $\phi_{nl}$ . In the case of the  $1s$  level the integral over  $q^2$  can also be evaluated analytically.

The muonic vacuum polarization (in which the  $e^+e^-$  loop is replaced by a  $\mu^+\mu^-$  loop) is evaluated by replacing the electron mass  $m_e$  by the muon mass in Eq. (16).

In order to achieve a few ppm accuracy, we also calculate the leading relativistic correction to the nonrelativistic electronic vacuum polarization contribution, which is done, in the framework of the Breit-Pauli approach, with the exact mass dependence, representing the interaction between the particles by the exchange of a massive photon. We integrate over this mass  $\varrho$  which is equivalent, through dispersion relation, to integrate over  $q$ . Following the derivation in Ref. [31] 83 that provides Eq. (8), but using  $\gamma_{\text{vp}}(r) = -\frac{\alpha}{r} e^{-\varrho r}$  instead of the Coulomb interaction, we get

$$V_{\text{vp}}^{\text{BP}}(r) = \frac{\alpha}{\pi} \int_4^\infty \frac{d(\varrho^2)}{\varrho^2} u\left(\frac{\varrho^2}{m_e^2}\right) \gamma_{\text{vp}}^{\text{BP}}(r) \quad (19)$$

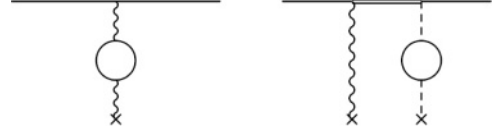


FIG. 3. Relativistic correction to vacuum polarization diagram. Dashed lines correspond to the Coulomb interaction, double line to the nonrelativistic propagator.

with

$$\begin{aligned} \gamma_{\text{vp}}^{\text{BP}}(r) = & \frac{Z\alpha}{8} \frac{1}{m_p^2} \left( 4\pi \delta^3(r) - \frac{\varrho^2}{r} e^{-\varrho r} \right) \\ & - \frac{Z\alpha}{4m_p m_\pi} \frac{\varrho^2 e^{-\varrho r}}{r} \left( 1 - \frac{\varrho r}{2} \right) \\ & - \frac{Z\alpha}{2m_p m_\pi} p^i \frac{e^{-\varrho r}}{r} \left( \delta_{ij} + \frac{r_i r_j}{r^2} (1 + \varrho r) \right) p^j \\ & + \frac{Z\alpha}{r^3} \left( \frac{1 + 2\kappa}{4m_p^2} + \frac{1 + \kappa}{2m_p m_\pi} \right) e^{-\varrho r} (1 + \varrho r) (\mathbf{r} \times \mathbf{p}) \cdot \boldsymbol{\sigma}. \end{aligned}$$

The Hamiltonian becomes  $H = H_0 + \delta H + V^{\text{BP}} + V_{\text{vp}} + V_{\text{vp}}^{\text{BP}} \equiv H_0 + W$ . We perform a perturbative expansion in  $W$  up to second order and keep only the main terms involving the massive photon. We get

$$\begin{aligned} E(\varrho) = & \langle \phi_{nl} | \gamma_{\text{vp}}^{\text{BP}} | \phi_{nl} \rangle \\ & + 2 \langle \phi_{nl} | (\delta H + V^{\text{BP}}) \frac{1}{(E_0 - H_0)} \gamma_{\text{vp}} | \phi_{nl} \rangle, \quad (20) \end{aligned}$$

which corresponds to the diagrams presented in Fig. 3. The reduced Coulomb Green function terms  $G' = \langle r_1 | \frac{1}{(E_0 - H_0)'} | r_2 \rangle$  are calculated using the code written for [19]. We finally integrate over the mass  $\varrho$

$$E = \frac{\alpha}{\pi} \int_4^\infty \frac{d(\varrho^2)}{\varrho^2} u\left(\frac{\varrho^2}{m_e^2}\right) E(\varrho). \quad (21)$$

### C. Two-loop vacuum polarization correction

The double vacuum polarization term (Fig. 4) corresponds to the shift:

$$E = \langle \phi_{nl} | V_{\text{vp}} \frac{1}{(E_0 - H_0)'} V_{\text{vp}} | \phi_{nl} \rangle. \quad (22)$$

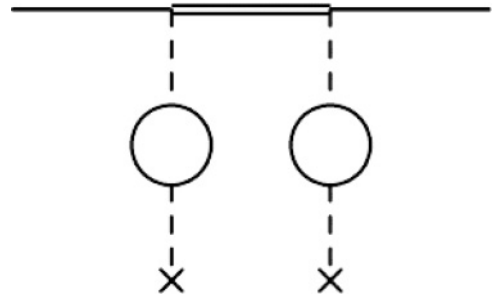


FIG. 4. Two-loop vacuum polarization diagram. See Fig. 3 for explanations of the symbols used.

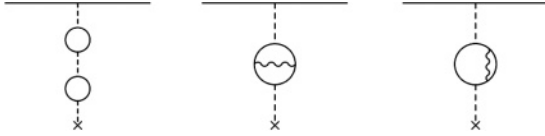


FIG. 5. Diagram corresponding to the Vacuum polarization at two loops (Källén and Sabry potential). See Fig. 3 for explanation of the symbols used.

Two-loop vacuum polarization (Fig. 5), known as the Källén and Sabry contribution [32], involves a modified photon propagator, in the same way as the one-loop one (14):

$$\bar{\omega}^{(2)}(-\mathbf{p}^2) = \left(\frac{\alpha}{\pi}\right)^2 \int_4^\infty d(q^2) \frac{-\mathbf{p}^2}{q^2(m_e^2 q^2 + \mathbf{p}^2)} u^{(2)}(q^2), \quad (23)$$

where the potential  $u^{(2)}(q^2)$  is given by [32]. We can proceed in a similar fashion as for the leading term, using Eq. (17), with

$$V_{\text{vp}}^{(2)}(r) = -\frac{Z\alpha}{r} \left(\frac{\alpha}{\pi}\right)^2 \int_4^\infty \frac{d(q^2)}{q^2} e^{-m_e q r} u^{(2)}(q^2). \quad (24)$$

We obtain

$$E = \langle \phi_{nl} | V_{\text{vp}}^{(2)} | \phi_{nl} \rangle = \int d^3r V_{\text{vp}}^{(2)}(r) |\phi_{nl}(\mathbf{r})|^2. \quad (25)$$

#### D. Finite size effects

The leading size correction due to the proton or the pion, for a  $ns$  level, from Eq. (9) is given in, e.g., [20] Eq. (51) as

$$\begin{aligned} \mathcal{E}_{NS}(Z\alpha, n) &= \frac{2}{3} \left(\frac{\mu_r}{m_\pi}\right)^3 \frac{(Z\alpha)^4}{n^3} m_\pi \frac{(r_p^2 + r_\pi^2)}{\lambda_C^2}, \\ &= 87.07547(58) \frac{Z^4 (r_p^2 + r_\pi^2)}{n^3} \text{meV}, \end{aligned} \quad (26)$$

where  $\lambda_C = 1.4138189$  fm is the pion Compton wavelength. The contribution of the proton to the shift is 61.710(99) meV using the proton charge radius from [22], 66.9(11) meV using [20] and 67.3(12) meV using [23]. The contribution from the pion is 39.32(94) meV, and largely dominates the uncertainty on this correction. This is to be compared with the uncertainty due to the pion mass, which represents, e.g., 5.3 meV on the  $2p - 1s$  transition.

The main corrections to the leading finite-size contribution are due to vacuum polarization, as illustrated by diagrams (a)



FIG. 6. Vacuum polarization correction to finite size effect diagrams. See Fig. 3 for explanations of the symbols used.



FIG. 7. Diagrams corresponding to the self-energies of pion and proton.

and (b) in Fig. 6, and are given by

$$E_a = -\frac{2}{3} \frac{\alpha}{4\pi} Z\alpha (r_p^2 + r_\pi^2) \int_4^\infty \frac{d(q^2)}{q^2} u(q^2) \times \int_0^\infty dr R_{nl}^2(r) [r(m_e q)^2 e^{-m_e q r} - \delta(r)], \quad (27)$$

$$E_b = 2 \left(\frac{2}{3} \pi Z\alpha\right) (r_p^2 + r_\pi^2) \times \int d^3r \phi_{nl}(\mathbf{r}) V_{vp}(r) G'(r, 0) \phi_{nl}(0). \quad (28)$$

#### E. Self-energy

Except for an unpublished internal report [33], we are not aware of any calculation of the pion self-energy. We include it here. This correction correspond to the diagrams in Fig. 7. In this calculation, the part due to the high-energy contribution (which corresponds to the particle form factor) is included in the finite size, as explained for the proton case in [34]. This part must not be included in the self-energy shift to avoid double counting. The remaining low-energy part is known [28] and does not depend on the particle spin value:

$$E_{\pi\text{SE}} = \frac{4}{3\pi n^3} \alpha (Z\alpha)^4 \frac{\mu^3}{m_\pi^2} \times \left\{ -\ln[k_0(n, l)] + \delta_{l,0} \ln \frac{m_\pi}{\mu(Z\alpha)^2} \right\}, \quad (29)$$

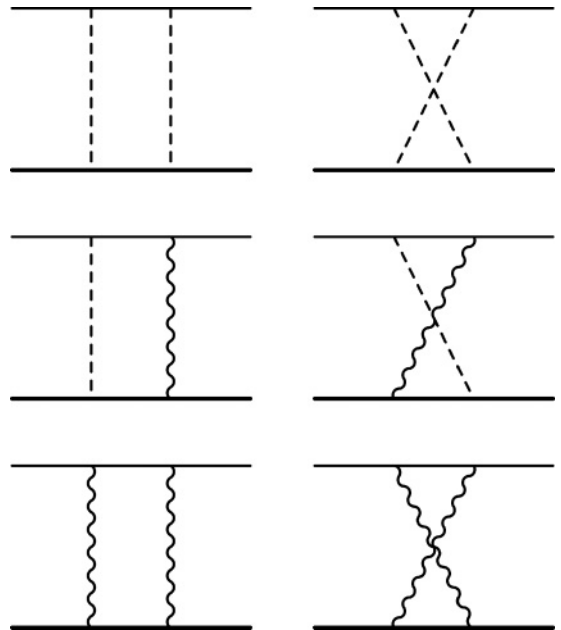


FIG. 8. Diagrams corresponding to the exchange of two photons. See previous figures for explanations.

TABLE I. Contributions to pionic hydrogen level energies (meV), sorted by size.  $F$  is the total angular momentum. Numbers in parentheses represent uncertainty in the last digits. When absent, the uncertainty is smaller than 1 in the last digit. The nonrelativistic energy is not shown. The proton and pion size corrections are given in Eq. (26).

Contribution	Eq.		1s	2p	3p	4p
VP one loop	(17)		-3240.802(16)	-35.79480(28)	-11.406601(86)	-4.920557(37)
Breit-Pauli interaction	(7)–(8)	$F = 1/2$	-178.46117(32)	-11.655153(37)	-4.220937(13)	-1.942614(6)
		$F = 3/2$		-4.048290(4)	-1.967051(3)	-0.991756(2)
Finite charge radius	(9)	$p$	61.710(99)	0	0	0
		$\pi^-$	39.32(94)	0	0	0
VP two loops (Källén & Sabry)			-24.36484(11)	-0.346025(3)	-0.107956	-0.046283
Pion self energy	(29)		5.656122(9)	0.003034	0.001144	0.000530
VP second order	(22)		-4.110407(25)	-0.008161	-0.002472	-0.001034
Relativistic corr. to VP	(21)	$F = 1/2$	-0.432480(2)	-0.026426	-0.008588	-0.003710
		$F = 3/2$		0.007631	0.002362	0.001008
VP corr. (b) to finite size	(28)	$p$	0.29779(48)	0	0	0
		$\pi^-$	0.1898(46)	0	0	0
Proton & pion polarization			-0.62(62)	0.000000	0.000000	0.000000
Muonic VP	(18)		-0.279306(2)	0.000000	0.000000	0.000000
Hadronic VP	(31)		-0.1874(42)	0.000000	0.000000	0.000000
Proton self energy	(29)		0.159247(2)	0.000067	0.000025	0.000012
VP corr. (a) to finite size	(27)	$p$	0.14573(24)	-0.000396	-0.000131	-0.000057
		$\pi^-$	0.0929(23)	-0.000253(7)	-0.000083(2)	-0.000036
two-photon exchange	(30)		-0.130157	-0.003483	-0.000959	-0.000390
Klein-Gordon correction	(10)		-0.024083	-0.000079	-0.000033	-0.000015
Total correction		$F = 1/2$	-3341.8(16)	-47.83168(32)	-15.746591(99)	-6.914155(43)
		$F = 3/2$		-40.19076(29)	-13.481756(89)	-5.958579(39)

where  $k_0(n, l)$  is the Bethe logarithm. The proton self-energy is obtained by replacing  $m_\pi$  by  $m_p$  and by multiplying the right-hand side of Eq. (29) by  $Z^2$  [19,34].

The finite size correction to the pion self-energy can be estimated from Ref. [20], Eq. (54). It is very small, even for the 1s level, and can be neglected at the present level accuracy.

### F. Additional recoil

We can go further, evaluating the pure recoil correction of order  $(Z\alpha)^5$ , calculated first by Salpeter [24], which correspond to two-photon exchange (Fig. 8). In our case, there is no theoretical framework for dealing with diagrams at this level of the perturbative expansion with overlapping strong and electromagnetic interactions. Since the strong interaction overlap with the electromagnetic one only at short distances [6], we have to exclude local interactions but keep

leading logarithmic parts of the contributions that would not overlap with the strong interaction. One can apply the formula from [35] which expresses the leading logarithmic term and an additional recoil term:

$$E = \frac{(Z\alpha)^5}{\pi n^3} \frac{\mu^3}{m_p m_\pi} \left\{ -\frac{2}{3} \ln(Z\alpha) \delta_{l,0} - \frac{8}{3} \ln[k_0(n, l)] - \frac{7}{6} n^3 \left\langle P \left( \frac{1}{(\mu\alpha r)^3} \right) \right\rangle_{nl} \right\}. \quad (30)$$

$P$  is a distribution function that subtracts the singularity at the origin [35].

### G. Hadronic QED corrections

Hadronic degrees of freedoms also contribute to the QED energy of the atom. Vacuum polarization loops with pions, for

TABLE II. Theoretical  $F$ -averaged energies of the emitted photon for  $np \rightarrow 1s$  transitions in pionic hydrogen ( $n = 2-4$ ) (eV). Numbers in parentheses: total uncertainty due to the uncertainties in the proton and pion charge radii (0.098 meV and 0.94 meV, respectively) and in the pion mass, combined quadratically. The transition energies from Ref. [7] are corrected for the pion mass value [21] ( $a \approx 4$  meV change). Our values include the contribution from the atom recoil when it emits the photon.

Transition	2p $\rightarrow$ 1s	3p $\rightarrow$ 1s	4p $\rightarrow$ 1s
Atomic recoil	-0.0027	-0.0038	-0.0043
This work	2429.5050(54)	2878.8303(64)	3036.0921(68)
Theor. [7]		2878.812(8)	3036.072(9)
Theor. [17]		2878.808(8)	
Exp. [17]		2885.916(13)(33)	
Exp. [18,47]		2885.928(8)	

TABLE III. Theoretical QED ground state energy and comparison with previous calculations.

1s-level QED binding energy	
This work	-3238.2867(78)
Ref. [3]	-3238.250
Ref. [7]	-3238.264(9)

example, or the proton polarization have pure electromagnetic effects that translate into small energy shifts. One must be careful, however, as in the correction described in Sec. II F, not to calculate the contribution in the region where the QED and strong interaction correction overlaps. The hadronic polarization correction has been evaluated for hydrogen [36,37], for muonic hydrogen by Borie [38,39], and more recently by Friar and coworkers [37] and Martynenko and Faustov [40–42], using experimental data from  $e^+ + e^- \rightarrow$  hadrons collisions. Here we use the relation

$$E_{\text{VP}}^{\text{Hadronic}} = 0.671(15)E_{\text{VP}}^{\mu} \quad (31)$$

from [37], to get  $-0.1874(42)$  meV.

We do not know of any proton polarization calculation for pionic hydrogen, but it has been calculated by several authors in muonic hydrogen [19,41–43]. Carlson and coworkers have very recently calculated this correction for both the hyperfine structure of muonic hydrogen [44,45] and for the  $2s$  Lamb shift [46]. The value provided in Ref. [41] for the  $1s$  state is  $0.144$  meV and  $0.018$  meV for the  $2s$ . Higher-order polarization corrections provided in [42] are negligible. Using the  $2s$  muonic hydrogen value from Ref. [46]  $\Delta E_{2s}^{pp} = -36.9 \pm 2.4 \mu\text{eV}$ , scaling it by  $n^3 = 8$  gives  $\Delta E_{1s}^{pp} = -295 \pm 19 \mu\text{eV}$ . We obtain the pionic hydrogen value by doing a scaling with the pion to muon reduced mass to the third power, we get a shift of order  $-0.62$  meV that we use with an uncertainty of 50%. There should be an additional contribution from the pion polarizability. To account for it we increase the polarizability error to 100% of the proton value.

### III. RESULTS

The numerical values of the corrections evaluated in Sec. II are presented in Table I, for  $1s$ ,  $2p$ ,  $3p$ , and  $4p$  states and relevant hyperfine sublevels. It should be noted that if hyperfine sublevels are statistically populated, the shift due to the hyperfine interaction averages to zero for transitions ending in an  $s$  state [48]. Adding the Schrödinger equation solution from Eq. (11) we obtain the transition energies presented in Table II, with an accuracy of  $\approx 2.4$  ppm, dominated by the uncertainties on the pion mass (2.2 ppm, for the  $3p \rightarrow 1s$

transition) and the charge radii (0.5 ppm). The energy of the photon emitted by an atom is slightly reduced, compared to the energy difference between the initial and final state, due to momentum and energy conservation: the atomic recoil consumes part of the available energy. Here, this correction is larger than our goal accuracy, due to the high energy of the emitted photon and low total mass of the atom. This correction is also included in Ref. [17]. The corresponding values are presented in Table II for an atom initially at rest, and added to the transition energies.

The values of the  $1s$  QED binding energy results are presented in Table III, together with previous evaluations. In all three tables, the uncertainties combines uncertainties due to the pion mass and to the pion and proton radii. These two sources of uncertainties, being uncorrelated, are added quadratically.

Using the present results and the experimental value from Ref. [17], Eq. (14), we obtain a strong interaction shift of  $-7.085 \pm 0.013(\text{stat.}) \pm 0.034(\text{syst.})$  eV, instead of  $7.108 \pm 0.013(\text{stat.}) \pm 0.034(\text{syst.})$  eV, using the theoretical value from Ref. [7]. This does not improve much the shift accuracy (0.75%), as it is dominated by the uncertainty in the pion mass, the transition energy being calibrated with electronic K x-ray transitions in Ar. Using the preliminary value from [18,47], which is calibrated with pionic oxygen transition energies, we get a shift of  $7.0977(64)(10)$  eV (instead of  $7.120$  eV), with a total relative accuracy of 0.09%. Because of this calibration method, which use an energy proportional to the pion mass, this new results depends only weakly on it.

In summary the present work uses nonrelativistic QED techniques to provide the most accurate evaluation of pure-QED transitions energies in pionic hydrogen. Combined with recent experimental values, it allows for a significant increase in the precision of the determination of the strong interaction shift and thus of the  $\pi^- p \rightarrow \pi^- p$  scattering length at low energy. Obtaining more accurate energies would require extending effective theories like the one described in [6] to evaluate strong and electromagnetic contributions to high orders, which is not currently possible, and an improved measurement of the pion mass. Deducing improved values of the isospin-independent scattering length from the shift would moreover require more accurate measurements of the low energy constant  $f_1$ .

### ACKNOWLEDGMENTS

Laboratoire Kastler Brossel is “UMR n° 8552” (CNRS, ENS, UPMC). Support from UPMC for a stay in Paris of K.P. is gratefully acknowledged. This work is also partially supported by Helmholtz Alliance HA216/EMMI. We thank D. Gotta for many suggestions including detailed suggestions on the manuscript and B. Loiseau, T.E.O. Ericson, and S. Wycech for helpful discussions.

- [1] S. Deser, M. L. Goldberger, K. Baumann, and W. Thirring, *Phys. Rev.* **96**, 774 (1954).  
 [2] J. Spuller, D. Berghofer, M. D. Hasinoff, R. Macdonald, D. F. Measday, M. Salomon, and T. Suzuki, *Phys. Lett. B* **67**, 479 (1977).

- [3] V. E. Lyubovitskij and A. Rusetsky, *Phys. Lett. B* **494**, 9 (2000).  
 [4] N. Fettes and U.-G. Meißner, *Nucl. Phys. A* **693**, 693 (2001).  
 [5] J. Gasser, M. A. Ivanov, E. Lipartia, M. Mojziz, and A. Rusetsky, *Eur. Phys. J. C* **26**, 13 (2002).

- [6] J. Gasser, V. E. Lyubovitskij, and A. Rusetsky, *Phys. Rep.* **456**, 167 (2008).
- [7] D. Sigg *et al.*, *Nucl. Phys. A* **609**, 310 (1996).
- [8] T. E. O. Ericson, B. Loiseau, and S. Wycech, *Int. J. Mod. Phys. A* **20**, 1650 (2005).
- [9] A. N. Ivanov, M. Faber, A. Hirtl, J. Marton, and N. I. Troitskaya, *Eur. Phys. J. A* **18**, 653 (2003).
- [10] G. C. Oades, G. Rasche, W. S. Woolcock, E. Matsinos, and A. Gashi, *Nucl. Phys. A* **794**, 73 (2007).
- [11] J. Gasser, V. E. Lyubovitskij, and A. Rusetsky, *Ann. Rev. Nucl. Part. Sci.* **59**, 169 (2009).
- [12] V. Baru, J. Haidenbauer, C. Hanhart, A. Kudryavtsev, V. Lensky, and U. Meißner, *ECONFC* **070910**, 127 (2007).
- [13] P. Hauser *et al.*, *Phys. Rev. C* **58**, R1869 (1998).
- [14] T. Strauch *et al.*, *Hyperfine Interact.* **193**, 47 (2009).
- [15] D. Chattelard *et al.*, *Nucl. Phys. A* **625**, 855 (1997).
- [16] H.-C. Schröder *et al.*, *Phys. Lett. B* **469**, 25 (1999).
- [17] H. C. Schröder *et al.*, *Eur. Phys. J. C* **21**, 473 (2001).
- [18] D. Gotta *et al.*, *Precision Physics of Simple Atoms and Molecules*, Lecture Notes in Physics, Vol. 745 (Springer, Berlin/Heidelberg, 2008), pp. 165–186.
- [19] K. Pachucki, *Phys. Rev. A* **53**, 2092 (1996).
- [20] P. J. Mohr, B. N. Taylor, and D. B. Newell, *Rev. Mod. Phys.* **80**, 633 (2008).
- [21] K. Nakamura and Particle Data Group, *J. Phys. G: Nucl. Part. Phys.* **37**, 075021 (2010).
- [22] R. Pohl *et al.*, *Nature (London)* **466**, 213 (2010).
- [23] A1 Collaboration, J. C. Bernauer, *et al.*, *Phys. Rev. Lett.* **105**, 242001 (2010).
- [24] E. E. Salpeter, *Phys. Rev.* **87**, 328 (1952).
- [25] W. A. Barker and F. N. Glover, *Phys. Rev.* **99**, 317 (1955).
- [26] J. L. Friar, J. Martorell, and D. W. L. Sprung, *Phys. Rev. A* **56**, 4579 (1997).
- [27] K. Pachucki, *Phys. Rev. A* **78**, 012504 (2008).
- [28] C. Itzykson and J.-B. Zuber, *Quantum Field Theory* (McGraw-Hill, New York, 1980).
- [29] E. A. Uehling, *Phys. Rev.* **48**, 55 (1935).
- [30] H. A. Bethe and E. E. Salpeter, *Quantum Mechanics of One- and Two-electron Atoms* (Springer-Verlag, Berlin, 1957).
- [31] V. Berestetskii, E. Lifshitz, and L. Pitaevskii, *Quantum Electrodynamics*, 2nd ed. (Pergamon Press, Oxford, 1982).
- [32] G. Källén and A. Sabry, *Mat. Fys. Medd. K. Dan. Vidensk. Selsk.* **29**, 17 (1955).
- [33] B. Jeckelmann, BIPA: Ein programm zur Berechnung von Bindungsenergien in pionischen Atomen, Technical Report ETHZ IMP LB-85-03 ( Institut de Physique de l'université de Fribourg, Suisse, 1985).
- [34] K. Pachucki, *Phys. Rev. A* **52**, 1079 (1995).
- [35] K. Pachucki, *J. Phys. B* **31**, 5123 (1999).
- [36] S. G. Karshenboim, *J. Phys. B* **28**, L77 (1995).
- [37] J. L. Friar, J. Martorell, and D. W. L. Sprung, *Phys. Rev. A* **59**, 4061 (1999).
- [38] E. Borie, *Z. Phys. A* **302**, 187 (1981).
- [39] E. Borie and G. A. Rinker, *Rev. Mod. Phys.* **54**, 67 (1982).
- [40] R. N. Faustov and A. P. Martynenko, *EPJ Direct* **1**, 1 (1999).
- [41] A. Martynenko and R. Faustov, *Phys. At. Nucl.* **63**, 845 (2000).
- [42] A. Martynenko and R. Faustov, *Phys. At. Nucl.* **64**, 1282 (2001).
- [43] K. Pachucki, *J. Phys. B* **32**, 137 (1999).
- [44] C. E. Carlson, V. Nazaryan, and K. Griffioen, *Phys. Rev. A* **78**, 022517 (2008).
- [45] C. E. Carlson, V. Nazaryan, and K. Griffioen, *Phys. Rev. A* **83**, 042509 (2011).
- [46] C. E. Carlson and M. Vanderhaeghen, [<http://arxiv.org/abs/1101.5965>] (2011), [arXiv:1101.5965](https://arxiv.org/abs/1101.5965).
- [47] M. Hennebach, Ph.D. thesis, Universität zu Köln, 2003.
- [48] M. Trassinelli and P. Indelicato, *Phys. Rev. A* **76**, 012510 (2007).